ISSN 0965-5441, Petroleum Chemistry, 2018, Vol. 58, No. 3, pp. 203–213. © Pleiades Publishing, Ltd., 2018.
Original Russian Text ©A.G. Dedov, A.S. Loktev, I.E. Mukhin, A.A. Karavaev, S.I. Tyumenova, A.E. Baranchikov, V.K. Ivanov, K.I. Maslakov, M.A. Bykov, I.I. Moiseev, 2018, published in Neftekhimiya, 2018, Vol. 58, No. 2, pp. 154–164.

Synthesis Gas Production by Partial Oxidation of Methane and Dry Reforming of Methane in the Presence of Novel Ni–Co/MFI Catalysts

A. G. Dedov[a], A. S. Loktev[a, *], I. E. Mukhin[a], A. A. Karavaev[a], S. I. Tyumenova[a], A. E. Baranchikov[b], V. K. Ivanov[b], K. I. Maslakov[c], M. A. Bykov[c], and I. I. Moiseev[a]

[a] *Gubkin Russian State University of Oil and Gas (National Research University), Moscow, Russia*
[b] *Kurnakov Institute of General and Inorganic Chemistry, Russian Academy of Sciences, Moscow, Russia*
[c] *Moscow State University, Moscow, Russia*
**e-mail: al57@rambler.ru, genchem@gubkin.ru*

Received September 11, 2017

Abstract—Catalysts based on Ni, Co, and NiCo supported on MFI zeolites for the partial oxidation of methane and dry reforming of methane to synthesis gas have been synthesized and studied. The total metal content in the catalysts is 2 wt %. A commercial zeolite with a binder (alumina) and a binder-free zeolite synthesized by an accelerated microwave-assisted hydrothermal method are used as supports. The synthesis gas yield is 97% in the presence of Ni and NiCo catalysts supported on the MFI zeolite synthesized by the microwave-assisted hydrothermal method. The simultaneous presence of Ni and Co in the catalyst makes the sample resistant to coking during dry reforming of methane, whereas the Ni catalyst is characterized by the formation of a significant amount of carbon fibers.

Keywords: synthesis gas, partial oxidation of methane, dry reforming of methane, cobalt, nickel, MFI zeolite, microwave-assisted hydrothermal synthesis

DOI: 10.1134/S0965544118030052

Synthesis gas ($CO–H_2$ mixture) is a key intermediate in the production of petrochemicals and hydrogen—a promising environmentally friendly fuel—from methane-containing feedstocks [1–8]. Partial oxidation of methane (POM) and dry reforming of methane (DRM) have a number of advantages over the currently available synthesis gas production processes based on steam reforming of methane. Advantages of POM are the process exothermicity and the composition of the resulting synthesis gas ($H_2/CO = 2$) that is favorable for the Fischer–Tropsch synthesis of hydrocarbons and methanol synthesis. The DRM process ($H_2/CO = 1$) is important from an environmental point of view because it contributes to the utilization of carbon dioxide, which is the main greenhouse gas. In addition, the DRM process can be based on the conversion of biogas, which is a renewable raw material.

Well-known POM and DRM catalysts are platinum group metals, nickel, and cobalt on oxide supports of various chemical origins [1–8]. In the presence of these catalysts, at about 1000°C, methane molecules begin to lose hydrogen atoms to generate intermediates, which form CO in the presence of an oxidizer (CO_2 and O_2 in the case of DRM and POM, respectively) and carbon deposits in the absence of an oxidizer. The two reaction products (CO and H_2) undergo oxidation more readily than the feed methane does. A rapid removal of these products from the reaction zone makes it possible to eliminate the wastage of carbon [6]. The activity of nickel-based catalysts is not inferior to that of platinum metals and is significantly superior to the activity of cobalt catalysts at relatively lower temperatures; however, nickel catalysts are prone to forming carbon deposits on their surface, particularly in DRM; these deposits not only block the active sites of the catalyst, but also lead to the clogging of the reactor.

An approach to solving these problems is the use of catalysts with a small size of active metal particles and a high specific surface area of the support [7]. Among the supports used for this purpose, an emphasis should be put on zeolites of various structures and zeolite-like mesoporous materials, which have a positive effect on the properties of nickel catalysts. In addition, the degree of coking of nickel catalysts can be decreased by admixing nickel with another component that will contribute to the oxidation of the surface carbon. One of these components is cobalt [9].

The deposition of 5–10 wt % Ni on the BEA zeolite leads to the formation of a POM catalyst which pro-

vides a quantitative yield of CO at 700–900°C [7]. The zeolite dealumination improves the catalyst stability; a decrease in the nickel content to 1 wt % leads to a significant decrease in the catalyst activity.

The 10%Ni/25%CeO_2–ZrO_2/ZSM-5 catalyst is active in POM even at 400°C; it provides a methane conversion of 50%. At 700°C, the methane conversion achieves 90% [10].

Various zeolite supports and a number of cocatalysts that contribute to a decrease in the degree of coking were tested in DRM. POM catalysts synthesized by calcination of a mixture of nickel nitrate or nickel, potassium, and calcium nitrates with the ZSM-5 zeolite (Si/Al > 200) containing 20% of alumina used as a binder were studied [11]. A nitrogen-diluted mixture of methane and CO_2 was fed into the reactor. In the presence of a 5.3 wt % Ni/ZSM-5 catalyst, the CO yield was 77% at 700°C; in this case, significant coking was observed. The addition of K and Ca led to a slight increase in the CO yield; however, coking was eliminated. A decrease in the Ni content in Ni/ZSM-5 to 2.4 wt % led to a decrease in the CO yield to 70% and elimination of coking. With an increase in the Ni content to 9.7 wt %, the CO yield increased to 83%, while coking became more significant. At 900°C, the KNiCa/ZSM-5 catalyst provided a quantitative yield of synthesis gas.

Nickel, cobalt, and mixed NiCo catalysts deposited on the ZSM-5 zeolite (Si/Al = 11.5) by impregnation were tested in DRM [12]. The metal content in the catalysts was 7 wt %. In a range of 600–800°C, close hydrogen yields (58–65%) were observed in the presence of these catalysts, except for the cobalt sample. In the presence of the cobalt catalyst, this hydrogen yield was achieved only above 700°C. However, this catalyst exhibited the highest CO selectivity at 600°C (68%). At 800°C, the CO selectivity of all the catalysts was approximately the same—at a level of 60–62%. It was found that the nickel catalyst was prone to coking; with respect to the methane and CO_2 conversion, it was inferior to the mixed nickel–cobalt catalysts. In general, the catalyst with Ni/Co = 0.5 was the most active and stable. At 800°C, the conversion of CO_2 and methane was 85 and 75%, respectively; the synthesis gas selectivity was 63%. The degree of coking was less than 1%.

The catalysts containing 5–7 wt % Ni supported on the Y zeolite exhibited higher activity in DRM than the activity of samples synthesized by the deposition of Ni on A, X, and ZSM-5 zeolites [13]. At 800°C, the methane and CO_2 conversion remained at a stable level of 92% for 5 h, while the hydrogen selectivity was 65%. The catalyst containing 3% Ni showed similar results at the beginning of the test; however, over time, the parameters decreased. It should be noted that less active catalysts were less prone to coking.

DRM results depend on the Si/Al ratio in Ni catalysts containing the NaZSM-5 zeolite and semicrystalline silica gel [14]. At 800°C, the best results were obtained in the presence of a catalyst containing 5 wt % Ni with Si/Al = 30; in this case, the conversion of CO_2 and CH_4 was 98 and 95%, respectively, at $H_2/CO = 0.91$.

The catalytic activity of nickel (1 wt %), platinum (0.5 wt %), and mixed nickel–platinum catalysts supported on the dealuminated FAU, Y, and BEA zeolites in DRM at 600–640°C was determined as the number of moles of methane converted per gram of metal per hour [15]. The mixed nickel–platinum catalysts were less active than the platinum samples, whereas the nickel catalysts were inactive and underwent severe coking. The best support was the dealuminated BEA zeolite; the activity of NiPtBEA and PtBEA was 1.9 and 3.2 mol/(g h), respectively.

At 700°C, a bimetallic Ni(2.5%)Rh(2.5%)/BEA catalyst [16] provided a methane and CO_2 conversion of 73 and 78%, respectively; the results were similar to those obtained in the presence of 5% Rh/BEA. However, the rhodium catalyst was not prone to coking, while the bimetallic sample contained 3% of coke after 2 h on-stream. The 5% Ni/BEA catalyst showed close initial conversion values for the reactants; however, it underwent rapid deactivation because of severe coking (7% coke after 2 h).

The addition of 0.1 wt % Rh to a 7.5% Ni/NaY DRM catalyst provided a 100% conversion of CO_2 and methane at 560–585°C [17].

Ultrasound irradiation of a catalyst containing cobalt supported on the H–Y zeolite made it possible to synthesize more active catalysts owing to an increase in the degree of dispersion of the cobalt particles [18]. A catalyst containing 10 wt % of cobalt provided a hydrogen and CO yield of 61 and 80%, respectively, at 850°C and 55 and 77%, respectively, at 750°C. However, the methane and CO_2 conversion values significantly decreased after 10 h on-stream.

Nickel–platinum catalysts supported on a silicalite of the MFI structure (also known as ZSM-5) and encapsulated in a silicate shell were tested in DRM [19]. A catalyst containing 1.5 wt % Ni with the addition of 0.5 wt % Pt showed a methane and CO_2 conversion of about 80% at 800°C; however, after 20 h on-stream, the conversion decreased to 60%. The platinum-free catalyst underwent deactivation much more rapidly. The catalysts that were not encapsulated in SiO_2 completely lost their activity after 1–6 h.

The authors of [20] synthesized Ni DRM catalysts using a silicate with the ferrierite (FER) zeolite structure, an MFI silicalite, and a silicate with an ordered mesoporous MCM-41 structure. The Ni content was 5 wt %. At 700°C, the catalysts showed comparable conversions of methane (63–77%) and CO_2 (83–90%); however, the best results were obtained in the presence of Ni/FER, which was stable for 30 h.

The use of a mesoporous SBA-16 silicate for the deposition of nickel led to the formation of an unstable DRM catalyst [21]. At the same time, at 700°C, the SBA-16-based catalyst containing 5 wt % Ni and 14.7 wt % Ce exhibited a stable methane conversion of 68–72%, a CO_2 conversion of 74–77%, and an H_2 selectivity of 85% for 100 h.

The authors of [22] synthesized DRM catalysts on the basis of mesoporous alumina; nickel and cerium were introduced at the hydrothermal synthesis stage. The nickel content was 7 wt %, while the cerium content in the cerium–alumina matrix was varied in a range of 1–4 mol %. It was found that the catalyst containing 1 mol % cerium was the most effective. At 800°C, the methane and CO_2 conversion achieved 85%, while the CO and H_2 selectivity was 95%.

The described literature data are not exhaustive; references in the cited papers contain data on a number of other studies of POM and DRM catalyzed by nickel-containing zeolite systems. However, the cited data elucidate the appropriateness of using these catalysts. In particular, effective supports are MFI materials exhibiting high thermal stability; in the literature, they are commonly referred to as ZSM-5 [10–14]. All the studied catalysts based on MFI zeolites, except for samples comprising platinum group metals, contained a significant amount of nickel (5 wt % and more); the zeolites were synthesized by the conventional hydrothermal method. The use of microwave treatment during the hydrothermal synthesis of MFI zeolites provides a significant acceleration of the crystallization process and the formation of materials with improved morphological characteristics [23, 24].

The aim of this study is to synthesize and test POM and DRM catalysts containing 2 wt % of nickel, cobalt, or a mixture thereof supported on an MFI zeolite synthesized by the microwave-assisted hydrothermal method. For comparison, similar catalysts supported on a commercial hydrothermally produced MFI zeolite containing alumina as a binder were studied. The use of POM and DRM catalysts based on an MFI zeolite containing less than 5 wt % of nickel and no platinum metal additives and catalysts based on an MFI zeolite synthesized by the microwave-assisted hydrothermal method has not been described in the literature.

EXPERIMENTAL

An MFI zeolite with a Si/Al molar ratio of 20 was synthesized by the microwave-assisted hydrothermal method [23] and transferred to the H form by ion exchange with ammonium nitrate and calcination of the ammonium form (hereinafter referred to as MFImw). An MFI zeolite in the H form with Si/Al = 38 containing 20 wt % of alumina as a binder, which was manufactured at OAO Novosibirsk Chemical Concentrates Plant by the conventional hydrothermal method, was used for comparison. The specific surface area was 325 m^2/g. Hereinafter, it is referred to as MFIht.

The zeolite fraction (0.5–1 mm) was dried at 300°C, weighed, and immersed in an aqueous solution containing calculated amounts of cobalt nitrate hexahydrate, nickel nitrate hexahydrate, or a mixture thereof providing 2 wt % of the metal in the catalyst subjected to drying and calcination at 500°C. The mixed nickel–cobalt catalysts contained 1 wt % of each of the metals; in the case of nickel and cobalt, this concentration approximately corresponds to equimolar amounts of the metals. Six catalyst samples were prepared; hereinafter, they are referred to as NiMFImw, CoMFImw, NiCoMFImw, NiMFIht, CoMFIht, and NiCoMFIht.

The phase composition of the catalysts was determined on a Rigaku MiniFlex 600 diffractometer (Japan) equipped with a detector with a graphite monochromator and a copper anticathode using Cu K_α radiation at $\lambda = 1.54187$ Å. The phase composition was determined using the International Center for Diffraction Data (ICDD) database.

The catalyst morphology before and after testing in POM and DRM was studied using a Carl Zeiss NVision 40 scanning electron microscope (SEM) equipped with secondary electron (SE or InLens) and backscattered electron detectors (ESB) at an accelerating voltage of 7 and 1 kV, respectively, and a magnification of up to 200000× and a JEOL JSM-6390LA SEM instrument (Japan) equipped a with secondary electron detector at an accelerating voltage of 5–25 kV.

The texture characteristics of the catalysts were determined by low-temperature nitrogen sorption on a Quantachrome AUTOSORB-1C/MS/TPR instrument. The results were processed using the Quantachrome AS1Win software package using the Brunauer–Emmett–Teller (BET), *t*-plot, Barrett–Joyner–Halenda (BJH), and nonlocal density functional theory (NLDFT) methods.

The catalytic properties of the samples in the POM and DRM reactions were studied in a heated flow-type quartz reactor with a thermocouple pocket. The end of the thermocouple was located in the middle of the catalyst bed. For the POM reaction, the free volume of the reactor was filled with quartz chips. The weight of the catalyst loaded into the reactor was 0.2 g; the pellet size was 0.5–1 mm. The reactor was fed with CH_4–O_2 or CH_4–CO_2 mixtures undiluted with an inert gas (manufactured at Moscow Gas Refining Plant; purity of 99.9%). The CH_4/O_2 ratio was 2; $CH_4/CO_2 = 1$; the flow rate of the gas mixtures was 11–12 and 15–16 L/(g cat h), respectively. The catalyst was heated to a predetermined temperature in a stream of a CH_4–O_2 or CH_4–CO_2 mixture for 1 h; after analysis, the temperature was increased or decreased to specified values. The product composi-

Table 1. Texture characteristics of the catalysts according to low-temperature nitrogen sorption data

Catalyst	S_{sp}[a], m^2/g	$S_{micropore}$[b], m^2/g	$V_{pore,\,total}$*, cm^3/g	$V_{pore\,dif.\,diam}$[c], cm^3/g		
				<1 nm	1–5 nm	5–50 nm
NiMFImw						
Original	371	367	0.195	0.131	0.027	0.014
POM	353	346	0.190	0.128	0.017	0.020
DRM	323	309	0.295	0.118	0.010	0.055
CoMFImw						
Original	376	375	0.196	0.134	0.025	0.012
POM	255	254	0.145	0.119	0.009	0.055
DRM	329	324	0.192	0.110	0.034	0.016
NiCoMFImw						
Original	380	379	0.194	0.135	0.025	0.012
POM	329	323	0.180	0.115	0.023	0.017
DRM	361	355	0.188	0.137	0.015	0.017
NiMFIht						
Original	345	269	0.326	0.106	0.032	0.130
POM	314	246	0.323	0.090	0.035	0.142
DRM	308	242	0.351	0.093	0.027	0.146
CoMFIht						
Original	347	274	0.322	0.106	0.033	0.130
POM	308	227	0.319	0.077	0.044	0.137
DRM	277	226	0.218	0.090	0.027	0.062
NiCoMFIht						
Original	339	274	0.326	0.102	0.034	0.124
POM	340	264	0.328	0.098	0.041	0.127
DRM	295	235	0.289	0.089	0.028	0.118

[a] Calculated by BET.
[b] Calculated by *t*-plot.
[c] Calculated by NLDFT.
* Determined at $P/P_0 = 0.99$.

tion was analyzed by chromatography as described in [9].

RESULTS AND DISCUSSION

All the samples based on the MFImw zeolite exhibited nitrogen adsorption–desorption isotherms characteristic of microporous MFI materials. It is evident that most of the pore volume and an even larger portion of the surface area are attributed to the presence of ultramicropores with a size of less than 1 nm (Table 1). In the adsorption isotherm, the presence of these micropores is evidenced by an abrupt absorption of nitrogen even at extremely low pressure. Owing to this feature, data on the pore sizes and surface cannot be obtained using nitrogen as an adsorbate. The only parameter that can be determined reliably is the volume of these pores. In addition, the shape of the adsorption–desorption isotherms suggests that the MFImw samples contain pores with a size of 2–5 nm. The volumes of micro- and mesopores of different sizes were determined by the NLDFT method. The shape of the adsorption–desorption isotherms suggests that the MFImw samples contain a negligible amount of mesopores.

The hysteresis observed for some samples is apparently attributed to the presence of poorly accessible micropores. This assumption is based on the increase in nitrogen absorption with decreasing pressure, which is observed in desorption isotherms for some MFImw samples. In fact, in this case, an equilibrium adsorption isotherm cannot be obtained; therefore, an additional "absorption" of nitrogen is recorded during desorption. In accordance with the recommendations of IUPAC and the established practice for microporous materials, calculations in the region of low rela-

tive pressures (<0.02 P/P_0) were conducted by the BET method.[1] In general, it should be noted that, for all the samples based on the MFImw zeolite, the total specific surface area, the specific surface area of micropores, and the volume of ultramicropores decreased after POM and DRM catalysis. However, the ultramicroporous structure remained dominant in the composition of the used samples; in general, this finding suggests that the texture of the catalysts is stable.

The catalysts based on the MFIht zeolite also have a significant specific surface area of micropores; however, the total pore volume in them is higher; this fact is apparently associated with the presence of a binder—alumina—in their composition. The determination of the volumes of micro- and mesopores by the NLDFT method suggests that the volume of pores with a size of more than 2 nm significantly increased. At the same time, it was found that the total volume of micro- and mesopores was two orders of magnitude lower than the total pore volume; this finding indicates the presence of a large volume of macropores and a developed outer surface. This assumption is supported by a significant difference between the total specific surface area and the specific surface area of micropores. The involvement in the POM and DRM catalysis led to a decrease in the total specific surface area and the specific surface area of micropores; however, it had a slight effect on the total pore volume and the volumes of micro- and mesopores.

The nature of the support and the supported metals significantly affected the results of the conversion of a methane–oxygen mixture by the POM process. In the presence of the NiMFImw and NiCoMFImw catalysts, the methane conversion and the synthesis gas yield achieved high values even at 800°C; in addition, the results did not change substantially with increasing temperature (Table 2). The obtained results are almost the same as those described in the literature [7, 10]; however, they were observed for catalysts containing a significantly lower amount of nickel. With a decrease in the nickel content from 5 to 1 wt %, the parameters of the NiBEA POM catalyst considerably decreased [7], whereas the NiCoMFImw catalyst containing 1 wt % nickel showed high values of methane conversion and synthesis gas yield in POM; this finding shows that the use of the MFImv zeolite as a support is advantageous.

It was found that the nickel-free CoMFImw sample was nonselective in POM. The methane conversion did not reach 40%; the hydrogen yield was negligible; the formation of large amounts of deep oxidation products (CO_2 and water), methane condensation products, coke, and resins was observed. However, it should be noted that the addition of cobalt to nickel led to an improvement of the POM results, rather than to worsening.

The replacement of MFImw by MFIht led to a significant worsening of the POM results in the presence of the NiMFIht nickel catalyst, which exhibited a behavior similar to that of CoMFImw. It was expected that the CoMFIht catalyst will show poor results in the tests; therefore, the catalyst was immediately heated to 950°C. This heating did not lead to a high synthesis gas yield. After subsequent cooling to 920 and 900°C, the hydrogen yield remained low; however, the methane conversion and the CO yield unexpectedly increased.

In the set of catalysts based on the MFIht zeolite, the mixed NiCoMFIht sample was the most selective. Heating to 900–950°C provided a synthesis gas yield of 60–65%. However, the catalyst was unstable; after the subsequent decrease in the POM temperature to 920 and 900°C, the results became worse than those observed at the same temperature during heating.

Thus, the MFI zeolite synthesized by the microwave-assisted hydrothermal method is more advantageous as a support for nickel and nickel–cobalt POM catalysts. The difference of the catalysts supported on this zeolite from the counterparts based on the commercial sample consists in the dominance of the microporous structure (Table 1); in addition, according to SEM, the catalysts have different morphologies (Fig. 1).

It is evident that the MFImw-based catalysts contain larger well-crystallized zeolite particles. Their surface contains nanoparticles comprising nickel and cobalt (light areas detected by backscattered electron imaging) and no significant carbon deposits. The MFIht-based catalysts contain smaller arbitrarily shaped zeolite particles.

Analysis of the diffraction patterns of the catalysts before and after POM (Fig. 2) showed that all of them exhibit intense reflections at $2\theta = 7°–10°$ and 22°–25° characteristic of MFI zeolites. Reliable identification of phases corresponding to nickel, cobalt, and their oxides is hindered because, at respective 2θ values, broad low-intensity reflections attributed to a small particle size are observed. However, it can be stated that the diffraction patterns of the original monometallic catalysts do not exhibit characteristic reflections of cobalt and nickel oxides; this finding can be associated with both a low metal content and a small oxide particle size.

The latter assumption is more reasonable because, after POM, reflections attributed to divalent nickel and cobalt oxides can be observed. The original bimetallic NiCoMFIht catalyst can contain the $NiCo_2O_4$ phase (possibly NiO). After POM, metal particles were not recorded in the diffraction patterns of the catalysts; this fact can be apparently attributed to small particle sizes or to cooling of the catalysts in a methane–oxygen mixture, which contributes to their oxi-

[1] In the case of microporous samples, the calculation of specific surface area by the BET method is always not entirely correct in terms of the BET theory.

Table 2. Results of methane partial oxidation

T, °C	Conversion CH_4, %	Yield, wt %			
		CO	H_2	CO_2	C_{2+}
NiMFImw					
800	95	92	92	2	0
850	97	95	95	1	0
900	97	97	97	Traces	0
920	97	95	95	Traces	0
950	97	95	95	Traces	0
CoMFImw					
800	28	8	4	18	Traces
850	36	10	3	18	1
900	37	10	2	14	4
920	33	9	2	7	7
950	35	11	3	11	6
NiCoMFImw					
800	93	89	86	4	0
850	97	93	91	2	0
900	98	97	97	1	0
920	98	97	97	1	0
NiMFIht					
800	25	6	3	18	0
850	29	9	2	15	1
900	31	12	2	12	1
920	33	13	3	12	2
950	33	17	4	9	3
CoMFIht					
950	34	16	4	10	5
920	80	67	4	1	0
900	80	66	4	3	2
NiCoMFIht					
800	20	7	3	11	1
850	22	12	4	63	3
900	43	35	29	7	1
920	70	65	60	5	Traces
950	70	64	58	4	Traces
920	35	26	14	7	2
900	28	19	6	6	3

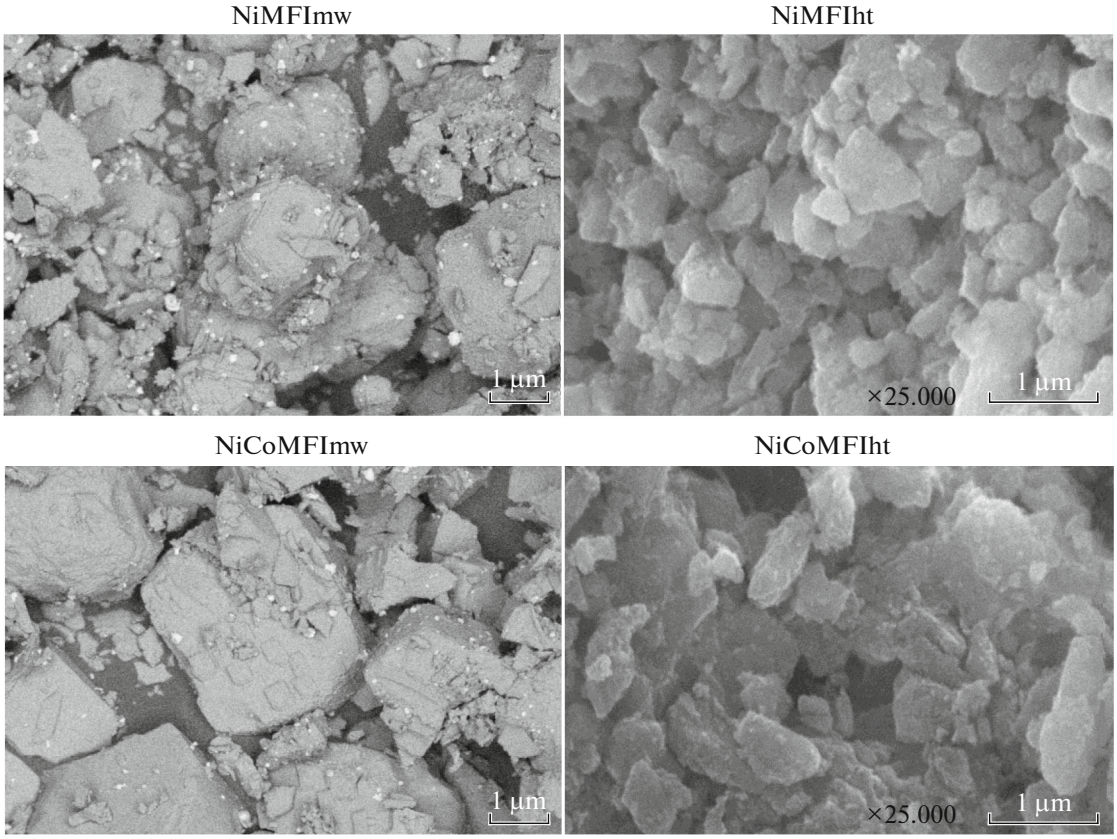

Fig. 1. SEM micrographs after POM catalysis.

dation. The spent catalysts did not exhibit ferromagnetic properties.

It was found that nickel-free CoMFImw was inactive and nonselective either in DRM (Table 3) so as in a series of POM tests. The conversion of methane and CO_2 did not exceed 40 and 60%, respectively; the hydrogen yield was significantly lower than the CO yield. The fact that the conversion of CO_2 is higher than that of methane and the yield of CO is higher than that of hydrogen can be attributed to the occurrence of the side reaction of CO_2 hydrogenation (reverse water gas shift reaction) [12]: $CO_2 + H_2 = CO + H_2O$. At the same time, in the presence of the NiMFImw and NiCoMFImw catalysts, high reactant conversion and synthesis gas yield values were achieved even at 800°C; in this case, the mixed NiCoMFImw catalyst showed the best results despite the fact that the nickel content in it was lower because of partial replacement of nickel by less effective cobalt.

An increase in temperature provided a nearly quantitative yield of synthesis gas. The observed synthesis gas yield values were almost the same as the literature data on the yields obtained in the presence of nickel catalysts supported on various zeolites with a significantly larger nickel content [11–22].

The replacement of MFImw by MFIht, which significantly worsened the results of POM in the presence of the NiMFIht nickel catalyst, conversely led to an improvement of the results in the case of DRM. In the presence of NiMFIht, the reactant conversion and the synthesis gas yield increased to values exceeding 90% with an increase in temperature from 800 to 950°C and decreased with subsequent cooling to 600°C. However, even at 700°C, the synthesis gas yield was close to 60%. It should be noted that, in the tests, an increase in temperature led to the suppression of CO_2 hydrogenation to CO, which is an undesired reaction; with the subsequent decrease in temperature, the vigorous occurrence of the reaction was observed.

According to expectations, the CoMFIht catalyst showed poor results in DRM tests; however, unlike the POM process, heating to 950°C provided a jump-like increase in the synthesis gas yield. After subsequent cooling to 800°C, the reactant conversion and the synthesis gas yield abruptly decreased.

The mixed NiCoMFIht catalyst is not inferior to the nickel counterpart in the DRM reaction; however, the contribution of the undesired CO hydrogenation reaction is more significant.

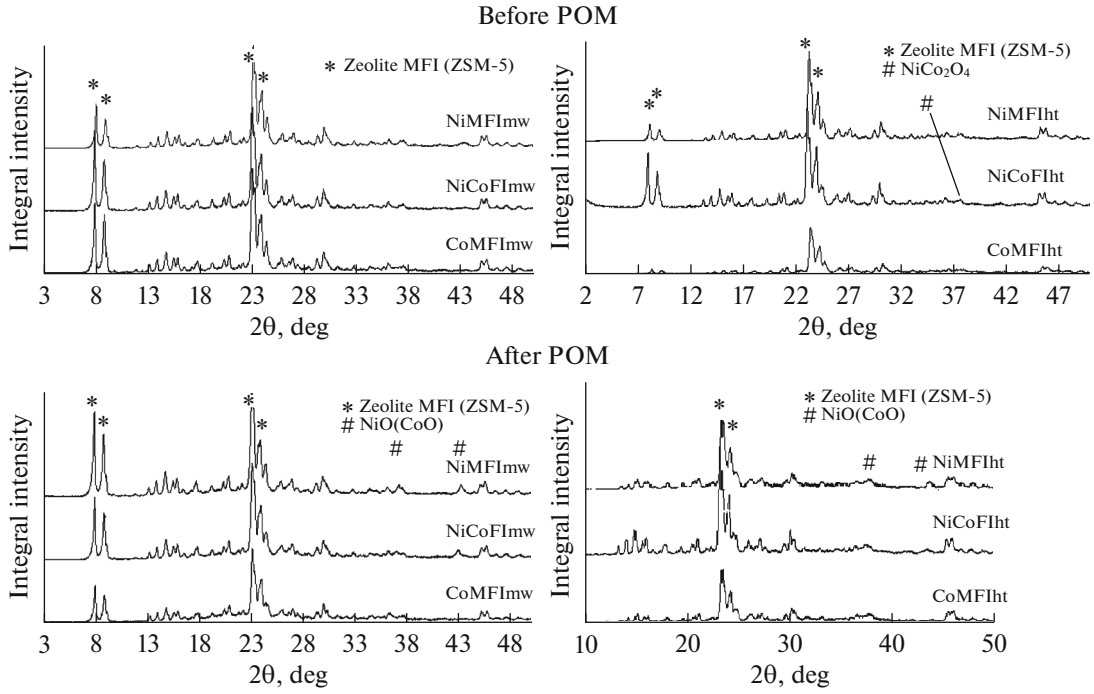

Fig. 2. Diffraction patterns of powders of the catalyst samples before and after POM.

SEM studies of the catalysts after DRM showed that the cobalt-free NiMFImw and NiMFIht samples underwent severe coking (Fig. 3).

The micrographs show carbon fibers or nanotubes with a thickness of 30–50 nm. The cobalt catalysts, which were ineffective in POM, did not undergo coking. The simultaneous presence of nickel and cobalt provided a significant decrease in the degree of coking of NiCoMFIht and completely eliminated coking in the case of NiCoMFImw.

The results show that the nickel-containing DRM catalysts based on the commercial MFIht zeolite are highly efficient in DRM; however, the use of nickel–cobalt catalysts supported on the MFImw zeolite synthesized by the microwave-assisted hydrothermal method makes it possible to eliminate catalyst coking, which is the main disadvantage of the DRM process.

The diffraction patterns of the catalysts after DRM (Fig. 4) preserved the reflections characteristic of MFI zeolites. It was impossible to reliably record reflections of metallic particles, apparently because the particles were small. Their presence in the nickel-containing catalysts after DRM is indirectly confirmed by the ferromagnetic properties of these samples (catalysts were well attracted to a magnet).

The diffraction pattern of CoMFImw, which is an inefficient DRM catalyst, exhibits reflections attributed to the formation of the Co_3O_4 phase. In the case of CoMFIht, this phase was not recorded. The diffraction pattern of the NiMFImw catalyst after DRM, as in the case of POM, exhibits reflections attributed to NiO. Their absence in the diffraction pattern of NiMFIht after DRM can be associated with the small sizes of these particles. The diffraction pattern of the bimetallic NiCoMFImw catalyst after DRM exhibits reflections that can be attributed to the formation of a Ni(II)–Co(III) mixed oxide phase; in the case of NiCoMFIht—the NiCoMFImw counterpart—the low-intensity reflection that apparently corresponds to the same phase present in the original sample is preserved (see Fig. 2).

Thus, on the basis of Ni, Co, and NiCo supported on the MFI zeolite synthesized by the microwave-assisted hydrothermal method and the commercial MFI zeolite, catalysts for synthesis gas production by POM and DRM have been synthesized and studied. The total metal content in the catalysts (2 wt %) is significantly lower than that described in the literature for analogous POM and DRM catalysts containing no platinum group metals. It has been shown that Ni and NiCo catalysts supported on the MFI zeolite synthesized by the microwave-assisted hydrothermal method provide a nearly quantitative yield of synthesis gas in the POM process; the same metals supported on each of the zeolites used are effective in DRM. The simultaneous presence of nickel and cobalt in a catalyst supported on the zeolite synthesized by the microwave-assisted hydrothermal method makes the catalyst resistant to coking during DRM, whereas the nickel

Table 3. Results of dry methane reforming

T, °C	Conversion, %		Yield, wt %	
	CH_4	CO_2	CO	H_2
		NiMFImw		
800	73	80	76	58
850	81	84	80	70
900	89	91	90	83
920	91	93	92	87
950	93	95	94	86
		CoMFImw		
800	3	15	0	2
850	6	23	3	4
900	17	40	28	8
920	28	50	37	10
950	40	59	49	13
		NiCoMFImw		
800	88	90	88	72
850	92	94	92	80
900	95	97	96	91
920	97	98	97	97
950	97	99	98	94
		NiMFIht		
800	81	81	80	81
850	89	89	85	86
900	92	92	91	92
920	93	93	92	93
950	94	94	92	94
800	77	87	87	88
750	79	85	75	78
700	61	72	63	57
650	44	56	44	38
600	24	37	25	19
		CoMFIht		
800	3	12	1	1
850	7	15	2	3
900	7	8	2	6
920	10	12	2	6
950	84	83	81	84
800	3	12	1	3
		NiCoMFIht		
800	90	92	89	76
850	96	96	95	80
900	98	98	97	91
920	98	98	97	87
950	99	99	98	88

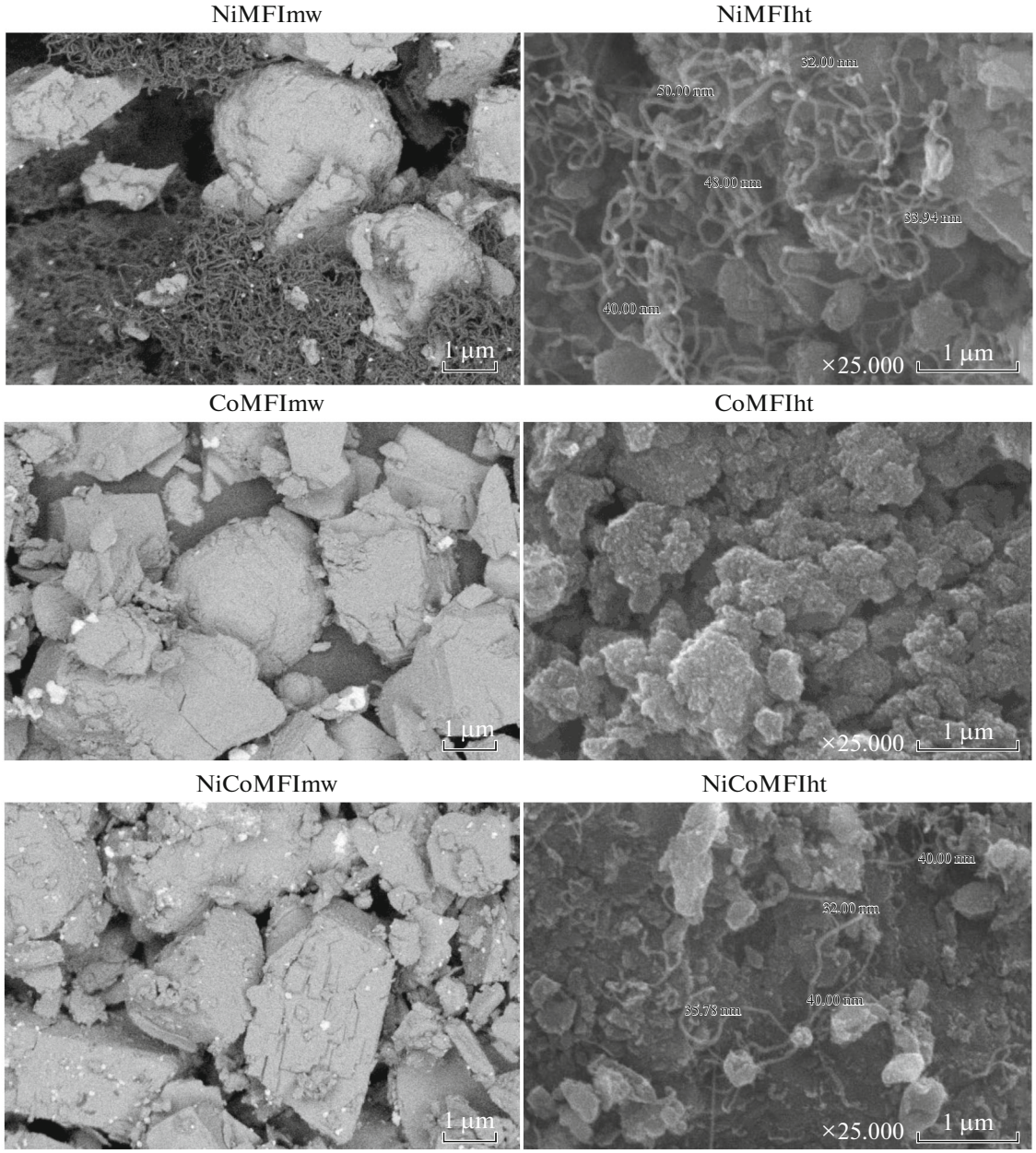

Fig. 3. SEM micrographs of the catalysts after DRM.

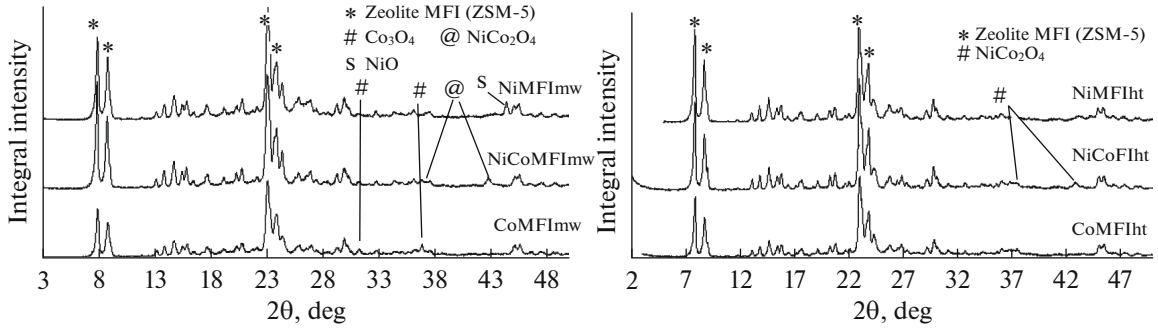

Fig. 4. Diffraction patterns of the catalyst powders after DRM.

catalyst is characterized by the formation of a significant amount of carbon fibers.

ACKNOWLEDGMENTS

The authors thank S.A. Chernyak (Moscow State University) for assistance in SEM studies. This work was supported by the Russian Science Foundation, project no. 14-13-01007P (catalyst synthesis, catalytic tests, pore structure analysis); the Ministry of Education and Science of the Russian Federation (basic part of the state task "Organization of Scientific Research," application form no. 1422); and the Presidium of the Russian Academy of Sciences.

REFERENCES

1. A. Holmen, Catal. Today, **142**, (2009).
2. B. C. Enger, R. Lødeng, and A. Holmen, Appl. Catal., A **346**, (2008).
3. S. Zeng, X. Zhang, X. Fu, et al., Appl. Catal., B **136/137**, 308 (2013).
4. *Methanol: The Basic Chemical and Energy Feedstock of the Future: Asinger's Vision Today*, Ed. by M. Bertau, H. Offermanns, L. Plass, (Springer, Heidelberg, 2014).
5. L. M. T. S. Rodrigues, R. B. Silva, M. G. C. Rocha, et al., Catal. Today **197**, 137 (2012).
6. V. S. Arutyunov, *Oxidative Conversion of Natural Gas* (KRASAND, Moscow, 2011).
7. K. A. Chalupka, W. K. Jozwiak, J. Rynkowski, et al., Appl. Catal., B **146**, 227 (2014).
8. A. G. Dedov, A. S. Loktev, D. A. Komissarenko, et al., Fuel Process. Technol. **148**, 128 (2016).
9. A. G. Dedov, A. S. Loktev, D. A. V. K. Ivanov, et al., Dokl. Phys. Chem. **461** (2), 73 (2015).
10. A. I. Osman, J. Meudal, F. Laffir, et al. Appl. Catal., B **212**, 68 (2017).
11. J.-S. Chang, S.-E. Park, and H. Chon, Appl. Catal., A **145**, 111 (1996).
12. J. Estephane, S. Aouad, S Hany., et al. Int. J. Hydrogen Energy **40**, 9201 (2015).
13. A. Luengnaruemitchai and A. Kaengsilalai, Chem. Eng. J. **144**, 96 (2008).
14. G. Moradi, F. Khezeli, and H. Hemmati, J. Nat. Gas Sci. Eng. **33**, 657 (2016).
15. A. N. Pinheiro, A. Valentini, J. M. Sasaki, and A. C. Oliveira, Appl. Catal., A **355**, 156 (2009).
16. P. Frontera, A. Aloise, A. Macario, et al., Top. Catal. **53**, 265 (2010).
17. J. Estephane, M. Ayoub, Kh. Safieh, et al., C. R. Chim. **18**, 277 (2015).
18. M. Abdollahifar, M. Haghighi, and M. Sharifi, Energy Conv. Manage. **103**, 1101 (2015).
19. C. Dai, S. Zhang, A. Zhang, et al., J. Mater. Chem. A **3**, 16461 (2015).
20. P. Frontera, A. Macario, A. Aloise, et al., Catal. Today **218/219**, 18 (2013).
21. S. Zhang, S. Muratsugu, N. Ishiguro, and M. Tada, ACS Catal. **3**, 1855 (2013).
22. N. Wang, K. Shen, L. Huang, et al., ACS Catal. **3**, 1638 (2013).
23. A. G. Dedov, A. S. Loktev, D. A. Levchenko, et al. Theor. Found. Chem. Eng. **49**, 502 (2015).
24. A. G. Dedov, A. S. Loktev, E. A. Isaeva, et al. Pet. Chem. **57**, 678 (2017).

Translated by M. Timoshinina